Development of a Standard Part System for Tie Rod Assemblies

João Miguel de Castro Francisco
joao.castro.francisco@tecnico.ulisboa.pt

Instituto Superior Técnico, Universidade de Lisboa, Portugal

January 2021

Abstract

With a surge in private jet aircraft flights, the business of aircraft interior design completion projects has increased. Supported by Jet Aviation, a company that performs and certifies these designs, the work developed aims to, in a first instance, develop a complete set of tie rod parts that can be mixed to form several assemblies. These tie rods connect the furniture designed to the fuselage, creating load paths to the aircraft structure. They are then used by Jet Aviation on a wide range of completion projects. The main steps covered on this work are the design constraints on the development of new tie rod segments, the analytical and computational calculations performed to obtain allowable loads and the experimental test executed on a tie rod sample. In fact, the main focus of this dissertation is to develop tensile allowable loads for the different parts, as well as compression allowable loads for the tubes. Consequently, the loads derived can be applied to reach a possible tie rod assembly allowable load. As such, analytical calculations are performed, which will be verified by finite element method computations. These allowable loads can be later employed to define margins of safety on projects which make use of them.

Keywords: Aircraft completion projects, Mechanical design, Static linear analysis, Tie rods, Allowable loads

1. Introduction

Over the last few years, air transportation has developed and occupied a defining place in the world economy. The number of passengers increased as this method of transportation became more accessible, which in turn made it possible for a faster industry development.

However, this past year has seen a decline on commercial flights. This is an impact caused by the coronavirus pandemic. This shifted the focus for private jet business, as wealthy flyers are prepared to pay a premium in order to avoid contact with other passengers on regular commercial flights [1]. In fact, private flights have shown a steeper recovery than commercial ones. This opens up a possibility for business. Very wealthy customers are open to pay for a customized interior design on their private aircraft.

Jet Aviation Basel is an approved Boeing and Airbus completions center, with capability to work on narrow and wide body aircraft models. In fact, Jet Aviation can provide this completion service due to the Design and Production Organization Approvals (DOA & POA) issued by EASA. The project completion engineering team works closely with the interior design, manufacturing and installation departments, in order to transform the initial conceptual design into an airworthy interior and a final aviation certified product.

This involves the modelling of cabinets and other required furniture, broadly named as monuments, followed by a linear static analysis performed by the engineering teams at Jet Aviation. The engineering team is entrusted with ensuring that technical feasibility and certification requirements are met, while providing custom solutions to meet said specifications.

After the monuments are produced in Jet Aviation wood shops, these are to be installed in the aircraft and tested both on the ground and in the air, to make sure the interior systems and cabinetry meets the certifiable requirements.

In fact, the commonly used installation method for high monuments' upper attachments is the use of a ceiling grid, as seen on Figure 1. The grid has the function of creating a load path between monuments and the OEM structure.

The mechanical connections between monuments and the ceiling grid, and between the ceiling grid and the OEM structure is assured by these links named tie rods.

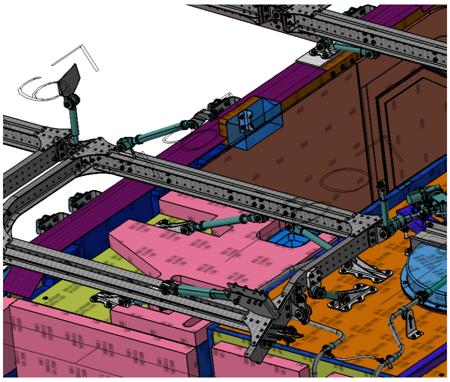

Figure 1: Example of upper monument attachments on the ceiling grid.[2]

For the majority of past completion projects, these parts were provided by a supplier, RO-RA Aviation Systems, according to a catalogue of tie rods developed with Jet Aviation. However, on what concerns one of the most recent completion projects performed on a Boeing 787 aircraft, these tie rods will not be used. Due to the composite nature of B787, a special coating treatment would have to be performed on the tie rods to protect these assemblies against corrosion, which could not be performed at the supplier's installations.

This led Jet Aviation to develop its own tie rod system for this project and to produce it on its own sheet metal shop. The work developed in this dissertation aims then to understand the possibility of achieving independence for tie rod production.

2. Background

A theoretical overview is done in order to set the necessary expressions used while developing the allowable loads for the tie rod part system, while some design constraints are also shown for the development of said parts. As to understand which required parts must be developed, a design overview is performed on previous aircraft ceiling grid modules, while presenting the current unfinished Jet Aviation tie rod solution.

2.1. Theoretical Overview

The tie rod parts will be analyzed under tension and compression. As such, for tension, a lug analysis needs to be performed on these parts, as well as analyzing their threaded and critical cross sections. As for compression, a buckling analysis is to be performed on the different tubes.

Before the theoretical formulas are presented, it is important to describe the material properties that will be required during the analysis for ST Steel RD 17-4PH H900 AMS 5643 and AL Alloy TUB 2024-T3 AMS 4088, the two materials that make up the tie rod parts, presented on Table 1.

Table 1: Material properties.[3]

Property	ST Steel RD 17-4PH H900 AMS 5643	AL Alloy TUB 2024-T3 AMS 4088
F_{tu} (ksi)	190	64
F_{ty} (ksi)	170	42
F_{bru} (ksi)	380	122
F_{bry} (ksi)	280	67
F_{cy} (ksi)	170	42
E (ksi)	28500	10500
E_c (ksi)	30000	10700
ε (%)	10	14

Under tension, it will be necessary to have the material's ultimate tensile allowable stress, F_{tu}; the yield tensile allowable stress, F_{ty}; the ultimate bearing allowable stress, F_{bru}; the yielding bearing allowable stress, F_{bry}; the Young's modulus, E; and the material's ultimate elongation, ε. Under compression, the yield compression allowable stress, F_{cy}, can be used, as well as the Young's modulus in compression, E_c.

The lug analysis method is based on the USAF Stress Analysis Manual (Ref. [4]), which can be applied to most lug joints. However, VVIP completion projects use isolators extensively. These components reduce the noise generated by metallic parts; however, they create a clearance between the pin and the lug hole. As such, correction factors, which come from pin-clearance data (Ref. [5]), need to be applied on the allowable loads obtained with this method.

Firstly, it is important to define the lug bearing strength, P_{bru_L}. The type of failure depends on the lug's radius, e, and thickness t, relative to the lug's hole diameter, D. The lug bearing strength is then calculated as follows, where (a) is to be used for shear tear-out if $t/D \geq 0.2$ and $e/D < 1.5$, while (b) for bearing for all other geometrical cases:

$$\begin{cases} P_{bru_L} = K_{br} \cdot a \cdot t \cdot F_{tu_{eff}} & \text{(a)} \\ P_{bru_L} = K_{br} \cdot D \cdot t \cdot F_{tu_{eff}} & \text{(b)} \end{cases} \quad (1)$$

where a is the lug edge ligament dimension, K_{br} is the axial bearing load coefficient and $F_{tu_{eff}}$ is the effective ultimate tension allowable stress.

Secondly, the lug net section strength under axial load, P_{nu_L} is then given by

$$P_{nu_L} = K_n \cdot (w - D) \cdot t \cdot F_{tu_{eff}}, \quad (2)$$

where w is the lug width and K_n is the net section tension stress coefficient.

Finally, a lug can also be subjected to transverse forces, so it is important to define the lug shear strength, P_{tru_L}, which is given by

$$P_{tru_L} = K_{tru} \cdot D \cdot t \cdot F_{tu_{eff}}, \quad (3)$$

where K_{tru} is the transverse load coefficient.

The lug allowable loads obtained with the previous formulas are only valid for a small clearance between pin and lug. For VVIP projects, the assembly used with isolators can be conservatively approximated in the same manner as an installation with pin clearance.

Stress concentration factors for axially loaded lugs with clearance-fit pins can be found in [5], for clearances of 0.2% and 100%. For intermediate clearances, the table values can be linearly interpolated to obtain the concentration factor.

The ratio between the concentration factors $K_{0.2}$, for 0.2% clearance, and K_c, for the actual lug clearance, can be used as the allowable reduction factor:

$$R = \frac{K_{0.2}}{K_c} \tag{4}$$

To perform bending analysis on the fork end parts of the tie rod, the Euler-Bernoulli beam theory is followed. Setting the stress equal to the ultimate bending stress F_{bu}, the allowable bending moment, M will be given by:

$$M = \frac{F_{bu} \cdot I}{y}, \tag{5}$$

where I is the cross section's inertia moment and y is the maximum distance to the cross section's neutral axis.

The allowable bending load, P_b, will then be given depending on the boundary conditions considered. For the case of fork arms, a boundary conditioned of guided end - fixed end was considered, which gives

$$P_b = \frac{2 \cdot M}{L} = \frac{2 \cdot F_{bu} \cdot I}{L \cdot y} \tag{6}$$

A buckling analysis will be important to perform on the tubes that compose the tie rod assemblies. In [6], this critical buckling load is given by

$$P_{cr} = \frac{c \cdot \pi^2 \cdot E_c \cdot I}{L^2}, \tag{7}$$

where L is the tube length and c is the fixity coefficient depending on the boundary conditions. The inertia moment, I, chosen must be the smallest one of the cross section.

2.2. Design Overview

In order to design a safe and reliable lug joint, several geometrical limitations can be imposed. These parameter ratio limitations have been used under service by different original equipment manufacturers. The recommended geometrical limitations were chosen from the boundaries set by Boeing and Airbus, ensuring the applicability of the lug analysis method and an efficient lug design, while still allowing some range for the mentioned geometrical ratios. They are presented on Table 2.

Table 2: Recommended lug design restrictions.

Parameter Ratio	Minimum	Maximum
t/D	0.20	1.25
w/D	1.25	3.00
e/D	0.75	3.00

Nevertheless, geometries that do not follow the recommended boundaries may be used after the appropriate analysis is performed on the impact the chosen dimensions have on the lug allowable, which must be done on a case-by-case basis.

The project performed on the Boeing 787 required the manufacture of Jet Aviation own set of tie rods.

This wide-body jet aircraft has an airframe primarily made of composite materials. Due to this reason, it was not possible to use the tie rods provided by the supplier, as a special coating would need to be applied to protect against corrosion.

This caused Jet Aviation to start developing their own set of tie rod parts for this specific project. The design of these parts was influenced by the RO-RA solution dimensions, the previous supplier.

As it can be seen on Figure 2, this is an example of one Jet Aviation tie rod configuration. These tie rods are made of several parts, and their main purpose is to transfer load axially between the two attachment points.

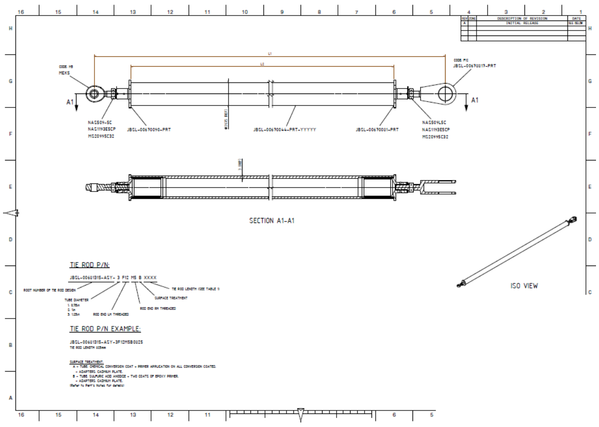

Figure 2: Example of a tie rod developed at Jet Aviation.[7]

Jet Aviation tie rods are composed by tubes which allow axial load transfer. The connection between tie rods and ceiling grid or OEM structure is guaranteed by the end parts installed on the tie rod. These are established joint connections, and fork ends act as the clevis of the joint, while rod ends will act as the fitting. The thread adapters are used to connect the fork or rod ends to the tube parts of the tie rod. These parts are necessary because they provide a link between the tube thread and the thread of the tie rod end parts. Nuts and locking devices are used as locking features, placed to reinforce the connection between the fork/rod ends parts and the thread adapters. These do not carry significant load and are therefore not analyzed.

To understand the required parts that still need to be developed internally by Jet Aviation in order to create a standardized system of tie rod assemblies, it was important to first analyze the previous completion projects that required the use of a ceiling grid.

In fact, a large variety of aircraft models from previous projects were analyzed so that it would be possible to gather information on the RO-RA tie rods used on the grids of these completion projects. From the grid modules of B737 and A319, it was possible to understand that a short tube with a built-in rod end was necessary to be developed, as well as some spatula ends for the B737 ceiling grid, as seen on Figure 3.

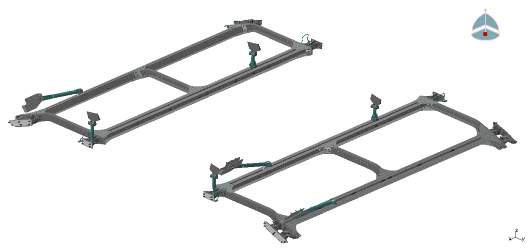

Figure 3: Standard grid module of B737.[7]

3. Implementation

An implementation of the design constraints defined is performed to design the missing parts that compose the Jet Aviation tie rod system. Secondly, all the parts are theoretically analyzed with the formulas previously presented, to derive values of allowable loads. Finally, a finite element study is conducted and its results are presented to consolidate the theoretical allowable results.

3.1. Developed Parts

The tie rod parts developed for B787 are capable of substituting the ones present on other aircraft, as they respect the dimensions of fittings and clevises used.

However, there are two parts that must be developed as they are required for a complete standard part system, as previously stated.

The short tube with a built-in rod end part will fulfill the role of a fitting on the joint connection. Named rod end RE05, it will also be manufactured in ST Steel RD, 17-4PH H900, AMS 5643, as the other tie rod end parts.

As it stands, it will require the use of a standard bearing MS14101-5, as most grid fittings do. This bearing allows the installation of pins and bolts with a diameter of 0.3125in.

To comply with the geometry ratios from Table 2, the other lug dimensions must be in the following range:

$$\begin{cases} 0.15 \text{ in} \leq t \leq 0.9375 \text{ in} \\ 0.9375 \text{ in} \leq w \leq 2.25 \text{ in} \\ 0.5625 \text{ in} \leq e \leq 2.25 \text{ in} \end{cases}$$

The final RE05 model is presented on Figure 4

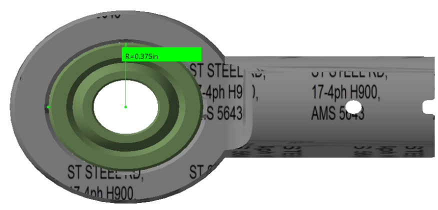

Figure 4: Design of rod end RE05.

As for the Spatula ends, they will also be manufactured in ST Steel RD, 17-4PH H900, AMS 5643, like other tie rod end parts.

In order not to change the joint connection parts (isolators and bushings) used on B737, the hole lug diameter of the spatula was set equal to 0.75in. As such, the previous dimension range applies to this lug as well.

The lug thickness and outer diameter dimensions were based on the previous spatula end used. As per Figure 5, these dimensions were set to $t = 9.1$mm and $e = 0.6$ in.

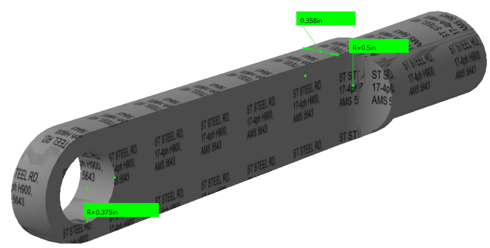

Figure 5: Jet Aviation spatula design.

As for the threaded section of the part that attaches to the tube, the dimensions were set equal to the ones used on the same region of the thread adapters. In fact, three different spatula ends were developed, as to be mounted on the three different type of tie rod tubes.

3.2. Allowable Theoretical Calculation

The theoretical formulas previously developed will now be applied to derive load allowable results for the loads that can be applied on each tie rod part that composes the standard part system, previously shown and developed.

The theoretical results for each part are presented on Table 3 below.

Table 3: Theoretical allowable tensile load of the tie rod parts.

Tie Rod Part	Theoretical Allowable (lbf)
Thread Adapter D = 0.75 in	13623
Thread Adapter D = 1.00 in	18782
Thread Adapter D = 1.25 in	24700
Fork End FE04	10432
Fork End FE05	10097
Fork End FE12	10097
Rod End RE05	19650
Spatula End D = 0.75 in	13623
Spatula End D = 1.00 in	17624
Spatula End D = 1.25 in	17624
Tube D = 0.75 in	8639
Tube D = 1.00 in	11781
Tube D = 1.25 in	14923

The thread adapters and tubes theoretical failure mode is related to the failure of their critical threaded cross section.

This failure mode also applies to fork end FE04 and the spatula end with D = 0.75; however the rest of spatula ends and the rod end RE05 show a theoretical lug failure mode. Finally, both fork ends FE05 and FE12 present a theoretical failure mode due to fork arm bending.

3.3. Allowable FEM Computation

To consolidate the theoretical allowable results previously calculated, finite element simulations were performed on the different developed parts that make up the tie rod assembly system.

The tensile analysis was performed on FEMAP, recurring to CTETRA elements with 10 grid points to model the solids. This element was chosen due to the complicated geometry of the tie rod parts. Using a midside node on the CTETRA elements' edges will improve their ability to deform and reduce their stiffness.

To apply the boundary conditions, two RBE3 elements and six DOF springs (one per degree of freedom) were used in order not to over constrain the CTETRA elements' nodes. As an example of a tensile analysis model represented on Figure 6, the RBE3 independent nodes on both elements correspond to the nodes present on the threaded surfaces of the solid. The dependent node of the RBE3 present on end B will have an applied load of 5000lbf. The other RBE3 element will have its independent node connected to one of the DOF springs node.

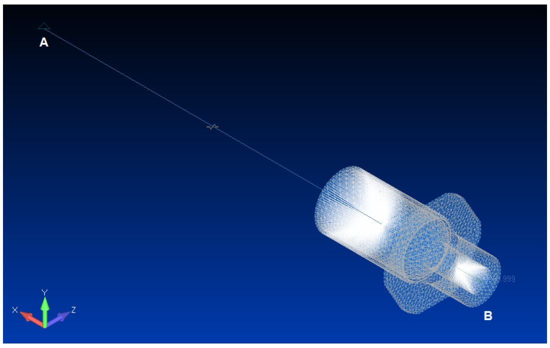

Figure 6: Tensile analysis modelling elements.

The fixed constraint on end A blocks all translation and rotation, and is applied only on the node of the DOF springs. These DOF springs will not affect the stress distribution on CTETRA elements as they do not divert the load path from the solid, making it an appropriate finite element modelling technique for this analysis.

The computational allowable results for each part were obtained by taking advantage of the linearity of the analysis, and are presented on Table 4 below.

Table 4: Computational allowable tensile load of the tie rod parts.

Tie Rod Part	Computational Allowable (lbf)
Thread Adapter D = 0.75 in	12314
Thread Adapter D = 1.00 in	15266
Thread Adapter D = 1.25 in	21146
Fork End FE04	9646
Fork End FE05	6988
Fork End FE12	6988
Rod End RE05	5581
Spatula End D = 0.75 in	10905
Spatula End D = 1.00 in	10556
Spatula End D = 1.25 in	10296
Tube D = 0.75 in	7382
Tube D = 1.00 in	10369
Tube D = 1.25 in	13287

While most theoretical failure modes were validated by these results, a possible new one was found for fork ends FE05 and FE12, rod end RE05 and the spatula ends.

This new failure mode involves the bending of the lug ligament, and is exemplified on Figure 7, which was not accounted for on lug analysis theoretical calculations.

This result could be a consequence of the way the RBE3 was modelled, distributing the applied load on the lug in a manner that simulates the pin clearance.

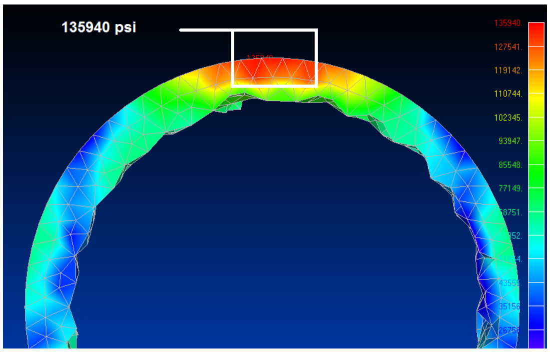

Figure 7: Lug ligament failure mode.

4. Results

An overview of the laboratory test is performed and its results are shown, followed by a discussion of the theoretical results compared with the computational and experimental results.

4.1. Laboratory Test

In order to consolidate the values calculated, a tensile failure test was performed on a tie rod sample.

The tie rod specimen tested was equipped with a tube of diameter $D = 0.75$ in. As seen on Figure 8, the tie rod ends installed were a fork end FE05 and a rod end MEK5 as representative of the majority of most connections present on the B787 project.

Figure 8: Tie rod sample tested until tensile failure.

A load cell was used to record the load. Before loading the sample, it was ensured that no constraints were applied on it.

The failure test was performed in 8 steps. For the first test, the load applied on the tie rod was 3000 lbf. Upon reaching the maximum applied load, the tie rod was held for 3 seconds under tension. Then the load could be released.

For the following tests, the maximum load was sequentially increased by 1000 lbf until either failure occurred or a load of 10000 lbf was reached. The procedure to hold the maximum load for 3 seconds was performed on all tests.

The results of the failure test are presented below.

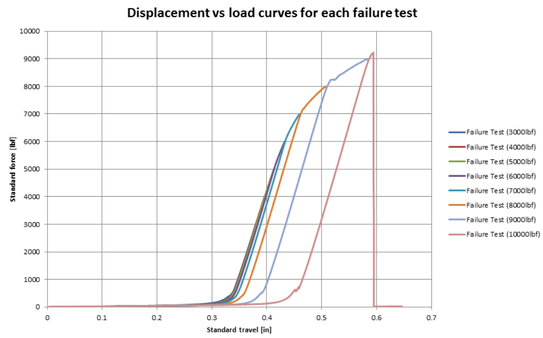

Figure 9: Tie rod sample failure test results.

As it is possible to understand from the results, the ultimate load the specimen was able to withstand under tension is 9230 lbf. After sample inspection, the failure occurred at the end of the threaded cross section of the tube.

4.2. Result Discussion

The failure test performed on the tie rod sample provided important information on the behaviour of the tie rod assembly under axial tensile load.

In fact, the specimen tested was composed by the following structural segments: a tube of diameter $D = 0.75$ in; a fork end FE12; a rod end MEK5; and two thread adapters. By the analysis performed, the expected first failure mode would happen due to the lug ligament bending of fork end FE12.

However, the fracture of the tube at the threaded cross section, for a tensile load of 9230 lbf, was the real failure mode of the assembly.

This failure mode allowable load was predicted by both computational and theoretical models to happen, respectively, at a tensile load of 7382 lbf and 8639 lbf. These predictions are appropriate, as they are close to the test value but still allow for a safe estimate.

A possible cause for this outcome resides in the fact that the bushing and isolator assembly installed on the joint connection might actually be amplifying the load transfer area from the pin to the lug.

If this is the case, the finite element model performed was too conservative, as the RBE3 was connected to the lug holes in such a way that would take into account pin clearance.

Despite of this underestimation of allowable loads for the developed parts, it is important to notice that the values of tensile load under which the tie rods will be subjected are also constrained by the other components of the joint installation.

That being said, the allowable loads for tie rod parts developed in this document could potentially be used to calculate margins of safety, as loads above 5000 lbf will never be applied on the tie rods.

5. Conclusions

Many achievements have been accomplished in this work, starting with the overview performed on previous projects' ceiling grids to verify if the B787 tie rod parts already designed could be repurposed for other aircraft, which was proven true.

Secondly, the design of important tie rod segments was performed in order to complete a set of parts that can be fully used on a large set of aircraft.

Thirdly, results for tensile allowable loads were derived in order to understand the maximum solicitation applicable on these parts. These results were then verified recurring to computational analysis.

Finally, the results of a tensile failure test performed on a sample are presented, which revealed that most of the allowable loads developed along this document were fairly conservative.

If followed, the results developed will most likely guarantee a proper functioning of Jet Aviation tie rods without the occurrence of failure. It was also explained that, due to connection issues, the loads under which the tie rods will be solicited will not reach the already conservative allowable values.

That being said, these results may be employed to derive safety margins on the completion projects that make use of the tie rod parts present on the document.

5.1. Future Work

For future work, some opportunities can be developed.

The first one is to perform more failure tensile tests on a wider range of tie rod assemblies. If several samples are tested until failure, it will be possible to derive allowable loads directly from the test results. As seen from the sample test destroyed, this test result is expected to be higher than the minimum value of each part that makes up the tie rod assembly.

The second one is to perform a cost analysis on the tie rod manufacture process in Jet Aviation' sheet metal shop. If this process is less expensive than buying directly from the supplier, than it should be implemented for future aircraft completion projects.

Acknowledgements

I want to express my appreciation to Professor Afzal Suleman for his availability to provide direction on the work developed.

Secondly, I would like to thank the stress team on which I was introduced for my traineeship in Jet Aviation. A special thanks to Anan Chen, Gianluca D'Alessandro and Romain Henot, my internship supervisors. The guidance, support and patience provided were crucial to make this dissertation.

Thirdly, I want to declare my appreciation to Jorge Moral Calvo and Jet Aviation for providing me with the required resources to perform this work. Thank you for the knowledge shared with me and for the guidance given in the beginning of my professional career.

References

[1] P. Georgiadis and A. Hancock, "Financial Times. "Private jets take off as wealthy flyers seek to avoid virus". 2020, October 25." Retrieved from https://www.ft.com/content/17282807-ab86-4333-b6c2-b8128f87fd4f. Accessed: 2020-12-15.

[2] "Stress Substantiation Report, Doc. No. JBSC-M-00156SSR-15, Issue 1." Jet Aviation, 2019.

[3] "MMPDS-12, "Metallic Materials Properties Development and Standardization", Federal Aviation Administration, year = 2017."

[4] G. E. Maddux, "AFFDL-TR-69-42, "USAF Stress Analysis Manual"," 1969.

[5] "ESDU 81006, Amendment A, "Stress concentration factors. Axially loaded lugs with clearance-fit pins"," 1981.

[6] M. C.-Y. Niu, *Airframe Stress Analysis and Sizing*. HongKong Conmilit Press LTD, 2^{nd} ed., 1999. ISBN:962-7128-08-2.

[7] Property of Jet Aviation.